UNIVERSITY OF CALIFORNIA SAN DIEGO

Detection of small synaptic signals in noisy electrophysiological data by means of artificial neural networks

A dissertation submitted in partial satisfaction
of the requirements for the degree Doctor of Philosophy

in

Neurosciences

by

Marc Joseph Marino

Committee in charge:

Professor Roberto Malinow, Chair
Professor Brenda Bloodgood
Professor Theresa Gaasterland
Professor Jeffry Isaacson
Professor Nicholas Spitzer

2020

The Dissertation of Marc Joseph Marino is approved, and it is acceptable in quality and form for publication on microfilm and electronically:

_____

_____

_____

_____

_____

Chair

University of California San Diego

2020

DEDICATION

I would like to dedicate this work to my family and friends who have supported me throughout this process, and particularly my mother and sister.

EPIGRAPH

Research in neurophysiology is much more like paddling a small canoe on a mountain river. The river which is fed by many distant springs carries you along all right though often in a peculiar direction. You have to paddle quite hard to keep afloat. And sooner or later some of your ideas are upset and are carried downstream like an upturned canoe.

Sir Alan Hodgkin, 1963.

The occurrence of the spontaneous subthreshold activity at an apparently normal synapse is of some general interest.

P. Fatt and B. Katz. Spontaneous subthreshold activity at motor nerve endings. J. Physiology,1952.

TABLE OF CONTENTS

Signature Page iii

Dedication iv

Epigraph v

Table of Contents vi

List of Figures vii

Acknowledgments viii

Vita ix

Abstract of the Dissertation x

Introduction 1

Chapter 1 Training the artificial neural network to detect mEPSC in noisy electrophysiological data 9

Chapter 2 Quantification of artificial neural network effectiveness at detection of mEPSCs 25

Chapter 3 Amplitude detection utilizing output features from the artificial neural network 37

Conclusion 47

LIST OF FIGURES

Figure 0.1: Various examples of electrophysiological waveforms: mEPSCs and mEPSPs.....3

Figure 1.1: Generation of training inputs from artificial mEPSC and noise.....13

Figure 1.2: Artificial neural network training methodology 16

Figure 1.3: Detection protocol: generation of a confidence value output 19

Figure 1.4: Detection of synthetic minis.....21

Figure 1.5: Detection of synthetic minis (magnification).....22

Figure 2.1: Receivers operating characteristic curve.....27

Figure 2.2: Receivers operating characteristic curve for varying amplitudes 29

Figure 2.3: True positive rate versus false discovery rate.....31

Figure 2.4: Artificial neural network performance comparison to human observer.....34

Figure 3.1: Amplitude Detection Paradigm.....39

Figure 3.2: Comparison between known and detected amplitudes.....41

Figure 3.3: Amplitude histograms of known and detected minis with noise distribution 42

Figure 3.4: Amplitude histograms of recordings before and after NBQX 44

ACKNOWLEDGEMENTS

I would like to acknowledge the Malinow lab for their support over 5 years I have been in the lab. I learned a multitude of techniques, in particular in-vitro imaging and electrophysiology. I would especially like to thank my principle investigator Roberto Malinow. I want to thank the post docs: Stephanie Alphonso, Kim Dore, Christophe Proulx, and Yifan Yu. Finally, I want to acknowledge my fellow graduate students who have assisted me throughout my time in the lab: Bradley Monk and Sage Aronson.

I would also like to acknowledge generous funding from the T32 Neuroplasticity of Aging training grant, the UC San Diego neurosciences department, and the National Institute of Health.

VITA

2011 Bachelor of Arts, University of Chicago

2014 Laboratory Technician, University of California San Diego

2020 Doctor of Philosophy, University of California San Diego

PUBLICATIONS

Ramachandran R, Marino MJ, Paul S, Wang Z, Mascarenhas NL, Pellett S, Johnson EA, DiNardo A, Yaksh TL. A Study and Review of Effects of Botulinum Toxins on Mast Cell Dependent and Independent Pruritus. Toxins (Basel). 2018 Mar 23;10(4). pii: E134.

Sikandar S, Gustavsson Y, Marino MJ, Dickenson AH, Yaksh TL, Sorkin LS, Ramachandran R. Effects of intraplantar botulinum toxin-B on carrageenan-induced changes in nociception and spinal phosphorylation of GluA1 and Akt. Eur J Neurosci. 2016 Jul;44(1):1714-22.

Park HJ*, Marino MJ*, Rondon ES, Xu Q, Yaksh TL. The effects of intraplantar and intrathecal botulinum toxin type B on tactile allodynia in mono and polyneuropathy in the mouse. Anesth Analg. 2015 Jul; 121(1):229-38. (*Co-first authors)

Marino M.J., Terashima T., Steinauer J.J., Eddinger K.A., Yaksh T.L., Xu Q. Botulinum Toxin B in the Sensory Afferent: Transmitter Release, Spinal Activation, and Pain Behavior. Pain. 2014 Apr; 155(4):674-84.

Marino M, Huang P, Malkmus S, Robertshaw E, Mac EA, Shatterman Y, Yaksh TL. Development and validation of an automated system for detection and assessment of scratching in the rodent. J Neurosci Methods. 2012 Aug 13; 211(1): 1-10.

ABSTRACT OF THE DISSERTATION

Detection of small synaptic signals in noisy electrophysiological data by means of artificial neural networks

by

Marc Joseph Marino

Doctor of Philosophy in Neurosciences

University of California San Diego, 2020

Professor Roberto Malinow, Chair

The miniature excitatory post synaptic current (mEPSC) is a fundamental electrophysiological measurement of quantal vesicular release of transmitter at synapses. Typically, for excitatory transmission at central nervous system neurons, due to the small size of the electrical signal relative to the noise, recordings containing mEPSCs are analyzed by eye in conjunction with a basic peak/template finding algorithm. Such methods require expertise and considerable time, and generally require elimination of signals smaller than ~8-10 pA to avoid counting noise (i.e. false positives). Here we describe an entirely automated approach to detect mEPSCs using a machine learning based tool. This method eliminates inter observer bias, and permits accurate detection of spontaneous mEPSCs smaller than 10 pA from brain slice neurons. Using whole cell recordings from the soma of CA1 hippocampal slice neurons this tool can detect more than 95% of mEPSCs identified by a trained human observer. Importantly, this tool identifies few events as mEPSCs in a recording of the same cell when excitatory

postsynaptic receptors are blocked, indicating a low false positive rate. Such recordings permit calculation of a true (96.6 ± 0.9%; n=10) and false (1.4 ± 0.1%; n=10) positive detection rate for mEPSCs. Using this new tool mEPSCs can be rapidly and accurately measured in an unbiased manner, and permits analysis of previously undetected mEPSCs.

INTRODUCTION

Miniature Excitatory Post Synaptic Currents (mEPSCs), are electrical currents recorded post synaptically via an intracellular recording electrode in a neuron receiving excitatory input (cite). These currents are thought to represent a quantal release of neurotransmitter, which are the smallest single unit of chemical transmission possible from one neuron to another. The first miniature excitatory post synaptic potentials were recorded by Fatt and Katz on the heels of the first intracellular recordings done by Hodgkin and Huxley (Hodgkin and Huxley,1952; Fatt and Katz, 1952). These quanta, it was subsequently discovered years after recording of the first miniature excitatory post synaptic potentials, are the release of a single vesicle containing neurotransmitter (Del Castillo and Katz, 1954; De Robertis EDPand Bennett, 1954; Whittaker et al., 1963; Diamond et al., 1995). Figure 1A shows an image of one of the first recordings of a mEPSP from the neuromuscular junction in the peripheral nervous system (Fatt and Katz, 1952). Vesicular release and the electrical signals elicited by them (mEPSPs or mEPSCs depending on the recording mode) represent a fundamental unit of transmission and therefore provide an observer a way to quantify the features of the neuron being recorded. mEPSC, themselves, have many characteristics including amplitude (size from baseline), rise time (time from baseline to reach peak), and frequency (distance between minis) (Auger and Marty, 1997; Simkus and Stricker. 2002). Using these characteristics an observer can make certain determination about one population of neurons versus another or between two neurons (Nicoll and Malenka, 1999). Observers can for example learn the quantal size, the release probability, Neurotransmitter Identity (Gaba mIPSC vs Glutamate mEPSC), and even make determinations whether there are presynaptic or post-synaptic changes occurring based on these recorded characteristics (Isaacson and Walmsley, 1995; Otmakhov, 1993; Shabel et al., 2014;Nicoll and Malenka, 1999). If one assumes the amount of glutamate in each vesicle is relatively fixed: increase in the amplitude of mEPSCs reflects increases in the function or number of AMPA receptors (or both) (Malinow, 2003; Malinow, 1991). Thus, since the 1950s minis have been an

electrophysiological waveform of interest to record and study. While recording equipment has improved signal to noise, electrophysiological data is inherently noisy (Malinow and Tsien, 1990; Carnevale and Hines, 2006; Kasdin, 1995), which makes it difficult to find small waveforms. This is the fundamental problem which this project attempts to address namely: detecting small mEPSC in noisy electrophysiological data utilizing novel artificial neural network (ANN) methodology.

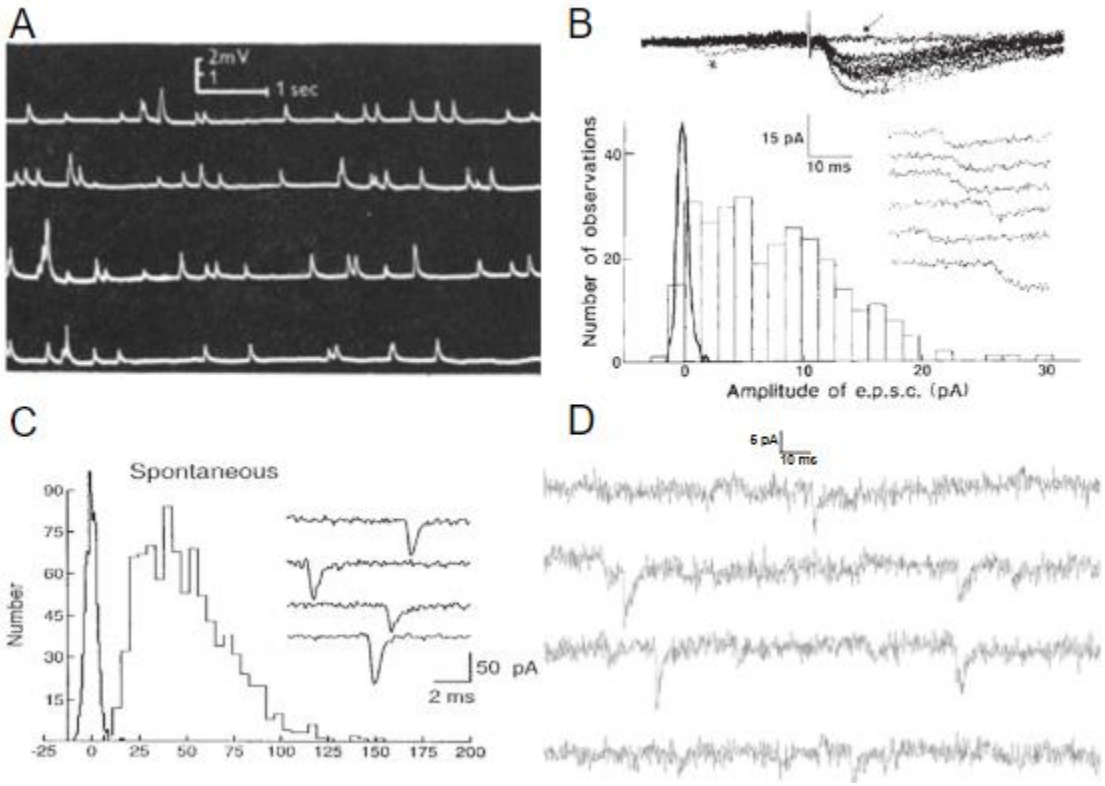

Figure 0.1. Example electrophysiological recordings of spontaneous or evoked mini EPSPs or mini EPSCs (minis) from peripheral and central nervous system and associated amplitude histograms A) The first spontaneous mEPSP recordings from peripheral nervous system, the muscle end plate (Fatt and Katz, 1952) B) Hippocampal slice of mEPSC and evoked events whole cell recordings top evoked and bottom spontaneous with amplitude and noise distributions (Malinow and Tsien, 1990) C) Recordings from the central nervous system of spontaneous mEPSC (right) and the amplitude distribution and noise distribution (left) (Isaacson and Walmsley, 1995) D) Typical hippocampal slice whole cell mEPSC electrophysiological recordings used in the training and testing of the artificial neural network mini detection software (Malinow Lab unpublished 2019).

The Problem of detecting mEPSC in noisy electrophysiological data

Analyzing spontaneous electrophysiological data has presented a problem since its initial conception namely: the signal must be substantially larger than the noise for a human observer to accurately and consistently detect and analyze any individual type of waveform. Typical examples of this issue are shown visually with traces and in amplitude distributions (figure 0.1 BCD). Figure 0.1 A for example shows both spontaneous (right) and evoked (top and left) electrophysiological data recorded in the Tsien lab (Malinow and Tsien, 1990). Notice that with evoked data (top and histogram) an observer is able to deduce much smaller amplitudes than with spontaneous data as the observer can deduce the exact point at which an evoked event peak should be located. Spontaneous data (right) is much more difficult to analyze and detect and therefore an amplitude threshold is normally set of between 5-10 pA depending on the noise of the data (often the threshold is 2 times the standard deviation of the noise). Central nervous system recordings from a large synapse that produces easily recognizable mEPSC can be seen in 0.1 C (Isaacson and Walmsley, 1995). Even in this special case where mEPSCs are often greater than 20 pA notice that these spontaneous recordings still utilize a cutoff threshold to eliminate noise that might contaminate the data. These factors have led us to seek a method for detecting minis (as seen in data recorded in the Malinow lab 0.1 D) that will not need to utilize an artificial amplitude threshold, but rather will be able to detect small waveforms even in noisy data.

Artificial neural networks: their advantages in detection and analysis of data

Artificial neural networks are a computational algorithm based loosely on a biological neural system (Hagan et al., 1996). The premise being that the artificial neural networks will enhance artificial computation of a given subject by utilizing some features of biological computation. Artificial neural networks are a series of connected nodes “neurons” with multiple layers (Hagan et al., 1996; Mathworks, 2020). Initially the input layer receives data and then connects to one or more hidden layer, which in turn connect to each other and then finally an

output layer. Data fed through the network will activate certain nodes because it holds the features that those nodes select for. If the data activates the correct pattern of nodes (after the network has been trained via gradient decent) then it will be passed as a positive result or alternatively be rejected (Moller, 1991). Other versions of networks allow for multiple outputs all following this basic method. What each node represents remains a mystery and thus the hidden layers of the network are called a “black box.” We can infer that nodes represent certain combinations of features of the input based on the connections being made and their strength, but we cannot make any definitive statements that the network is selecting for X feature of the input data (Google, 2013; Sejnowski, 2020). Although not knowing how a computational method operates is an unfortunate drawback this is more than made up for by the excellent results (Sejnowski, 2020). Other attempts to solve the problem of mini detection include deconvolution methods from the Jonas Lab that attempt to reduce signal to noise (Pernía-Andrade et al., 2012). Others have attempted to recognize a pattern using templates (Ankri, 1994; Richardson, 2008; Clements and Bekkers, 1997; Shi, 2009). Artificial neural networks, however, superseded them in its effectiveness, speed, and most importantly their ability to generalize. This generalization, effectively the capability to learn that similar patterns can be grouped together, is the real strength of the ANN and allows for our method to succeed.

Aims of project

The aims of the project are threefold. First, we wanted a computational system that could detect small minis previously unobserved or that are unobservable by the human eye. Although various groups have previously been able to observe at analyze small minis from evoked samples, we were interested in seeing if we could detect such small minis e.g. <5-8 pA reliably in spontaneous recordings. Second, we wished to improve speed, reliability, and overall performance compared to human observation. Human observation is both bias and difficult when analyzing mEPSC. Even with the help of current computational tools our and other labs still often required human observers to manually check and analyze detected data. Third and

finally, we wanted a system that could accurately characterize the detected mEPSC. This is critical considering our first aim is to detect such small mEPSC. Overall, the desire with this method and project is to provide a conceptual framework for others to utilize ANN to detect and analyze waveforms in their electrophysiological data. ANN are a powerful tool for detection and analysis, and we have shown here that they can be used very successfully to assist researchers in their data analysis.

References

Ankri, N., P. Legendre, H. Korn. 1994. Automatic detection of spontaneous synaptic responses in central neurons. J. Neurosci. Methods. 52:87–100

Auger, C., and Marty A.. 1997. Heterogeneity of functional synaptic parameters among single release sites. Neuron. 19:139–150.

Carnevale, N. T., and Hines M. L.. 2006. The Neuron Book. Cambridge University Press, Cambridge. 25. DeFelice, L. J. 1981. Introduction to Membrane Noise. Plenum Press, New York.

Clements, J. D., and J. M. Bekkers. 1997. Detection of spontaneous synaptic events with an optimally scaled template. Biophys. J. 73:220–229.

De Robertis EDP, Bennett HS (1954). "Submicroscopic vesicular component in the synapse". Fed Proc. 13: 35.

Del Castillo JB, Katz B (1954). "Quantal components of the endplate potential". J. Physiol. 124 (3): 560–573.

Diamond, J. S., and C. E. Jahr. 1995. Asynchronous release of synaptic vesicles determines the time course of the AMPA receptor-mediated EPSC. Neuron. 15:1097–1107.

Fatt, P., and B. Katz. 1952. Spontaneous subthreshold activity at motor nerve endings. J. Physiol. 117:109–128.

Gray EG, Whittaker VP (1962). "The isolation of nerve endings from brain: an electron microscopic study of cell fragments derived from homogenization and centrifugation". J Anat. 96: 79–88.

Google Research, “TensorFlow: Large-scale machine learning on heterogeneous systems,” 2013.

Hagan M.T., Demuth H.B., & Beale M.H., Neural Network Design, Boston, MA: PWS Publishing, 1996, Chapters 11 and 12.

Hodgkin AL, Huxley AF (August 1952). "A quantitative description of membrane current and its application to conduction and excitation in nerve". The Journal of Physiology. 117 (4): 500–44.

Isaacson JS, Walmsley B. Counting quanta: direct measurements of transmitter release at a central synapse. *Neuron*. 1995;15(4):875-884.

Kasdin, N. J. 1995. Discrete simulation of colored noise and stochastic processes and 1/fa power law noise generation. Proc. IEEE. 83: 802–827. Biophysical Journal 103(7) 1429–1439 1438 Pernı´a-Andrade et al.

Malinow R, Tsien RW. Presynaptic enhancement shown by whole-cell recordings of long-term potentiation in hippocampal slices. *Nature*. 1990;346(6280):177-180.

Malinow R. Transmission between pairs of hippocampal slice neurons: quantal levels, oscillations, and LTP. *Science*. 1991;252(5006):722-724.

Malinow R, Malenka RC. AMPA receptor trafficking and synaptic plasticity. *Annu Rev Neurosci*. 2002;25:103-126.

Malinow R. AMPA receptor trafficking and long-term potentiation. Philos Trans R Soc Lond B Biol Sci. 2003;358(1432):707-714.

Moller MF. “A scaled conjugate gradient algorithm for fast supervised learning,” Neural networks, 1991.

Multilayer Shallow Neural Network Architecture. www.mathworks.com. Retrieved 18th April 2020. www.mathworks.com/help/deeplearning/ug/multilayer-neural-network-architecture.html

Nicoll RA, Malenka RC. Expression mechanisms underlying NMDA receptor-dependent long-term potentiation. *Ann N Y Acad Sci*. 1999; 868:515-525.

Otmakhov N, Shirke AM, Malinow R. Measuring the impact of probabilistic transmission on neuronal output. *Neuron*. 1993;10(6):1101-1111.

Pernía-Andrade A.J., Goswami S.P., Stickler Y., Fröbe U., Schlögl A., Jonas P. A deconvolution-based method with high sensitivity and temporal resolution for detection of spontaneous synaptic currents *in vitro* and *in vivo*. Biophys. J. 2012;103:1429–1439.

Richardson, M. J. E., and G. Silberberg. 2008. Measurement and analysis of postsynaptic potentials using a novel voltage-deconvolution method. J. Neurophysiol. 99:1020–1031.

Sejnowski TJ. “The Unreasonable Effectiveness of Deep Learning in Artificial Intelligence.” Proceedings of the National Academy of Sciences, 2020, pii. 201907373.

Simkus, C. R. L., and C. Stricker. 2002. Properties of mEPSCs recorded in layer II neurones of rat barrel cortex. J. Physiol. 545:509–520.

Shabel SJ, Proulx CD, Piriz J, Malinow R. Mood regulation. GABA/glutamate co-release controls habenula output and is modified by antidepressant treatment. *Science*. 2014;345(6203):1494-1498.

Shi, Y., Z. Nenadic, and X. Xu. 2010. Novel use of matched filtering for synaptic event detection and extraction. PLoS ONE. 5:e15517. 37. Daw, M. I., L. Tricoire, ., C. J. McBain. 2009.

Whittaker VP, Michaelson IA, Kirkland RJ (1963). "The separation of synaptic vesicles from disrupted nerve ending particles". *Biochem Pharmacol*. 12 (2): 300–302.

Whittaker VP, Michaelson IA, Kirkland RJ (1964). "The separation of synaptic vesicles from nerve ending particles ('synaptosomes')". *Biochem J*. 90 (2): 293–303.

CHAPTER 1: Training the artificial neural network to detect mEPSC in noisy electrophysiological data

Introduction

In order to detect mEPSC in noisy electrophysiological data using an artificial neural network, the network must be trained to do so (Sejnowski, 2020; Google Research 2013; Hagan, 1996). This chapter will describe in detail a novel method of producing a training set and utilizing this training set to effectively train a standard artificial neural network. One of the key difficulties in using artificial neural networks has been the need to manually annotate datasets in order to train them. This annotation consists of a human observer manually marking samples to build up a target set (Van Eycke, 2019). In this case, electrophysiological waveforms would need to be identified and marked as positive mEPSC and other noisy electrophysiological waveforms as negative. This limits the neural network only to what a human eye can identify in noisy electrophysiological data (usually 8-10 pA minimum mEPSC Isaacson and Walmsley, 1995; Malinow and Tsien, 1990). Further, neural networks improve with the more input training data provided, thus the need for human identification hinders the overall quality of the network (Sejnowski, 2020; Van Eycke, 2019). This manually annotated target set would then be used by the neural network to train itself to correctly identify mEPSC. In order to remove this time consuming step and provide a more rigorous and flexible system of training, our algorithm utilizes a new approach to training a neural network using “artificial mEPSC” and real noisy electrophysiological data from the recording under analysis (see Figure 1.1). These two components are digitally added producing a training set of events. Rather than having to identify thousands of real minis, our system instead uses a template of 10 averaged minis chosen by an observer that most closely match the mEPSC waveform found in their recordings (see Figure 0.1 B,C,D in introduction to see examples of recorded mEPSC). One advantage is that this allows for extreme specialization of the network for an individual observer’s recordings, for example if gaba mIPSCs versus glutamate mEPSCs needed to be detected preferentially, or if

an observer's mEPSC had a faster or slower time course on average. It should be made clear, however, that this is not a template matching algorithm, which would require the found minis to match the exact chosen templates. Instead, these chosen average minis are merely used to construct "synthetic minis." These synthetic minis will become part of a much larger training set which will be used by the network to train itself to identify a generally similar shaped waveform (Hagan, 1996; Moller, 1991). In a matter of seconds 10,000 training set minis and 10,000 training set noise samples can be generated for the training of the artificial neural network. This novel approach to training artificial neural networks provides flexibility to the observer, faster results, improved accuracy, and finally the ability to detect minis that no human eye would be able to discern.

Materials & Methods

Figure 1.1 represents visually how a synthetic mini waveform is linearly summed with electrophysiological noise chosen randomly from the recording under analysis to form a final training set waveform. In order to generate a synthetic mini (Figure 1.1 A) the template mEPSC, a synthetic mini is generated by averaging 10 human observed mEPSC from electrophysiological recordings containing TTX in order to block action potentials (Malinow and Tsien, 1990). The amplitude of this smooth synthetic mini is set to 1 pA. This final template will be further modified prior to being linearly summed with noise. Two variables of the template are changed: its half width and its amplitude. The training template mEPSCs before being digitally added noise will have amplitudes following a Pearson distribution, which most closely mimics the observed distribution of recorded mEPSC (Bekkers et al., 1990; Isaacson and Walmsley, 1995; Paulsen and Heggelund, 1996), with an average of 10 pA. A reference Pearson distribution generated in Matlab has been shown as compared to a gaussian "normal" distribution (Figure 1.1 D). Other amplitude parameters were attempted with less successful implementation, including fixed uniform distributions. The average amplitude size of the distribution was also modified, a 10 pA average performed the best for our recordings, but this

may not be the case for all recordings. This and other parameters may be modified in future versions of this algorithm or by individual users based on results with their own differing data sets. The half width of each synthetic mini is then randomly stretched according to the formula 1/ (.3+.7*rand), where rand is a computationally randomly selected number from 0-1; and the extremes are 1/.3 and 1. This creates a training set with a variety of amplitude and width minis which follow the original general shape of the template, but which critically provide a dynamic range of minis from which the artificial neural network can learn. Most importantly all of these synthetic minis are aligned so that their peak amplitude is found at point number 60 out of the 160 point time series. This ensures that the artificial neural network will preferentially recognize only mEPSC that are found with their peaks at this point in the time series. The creation of the synthetic minis provides a novel way to train an artificial neural network without the need for the same lengthy human intervention usually required. Further, this method allows for the exposure to the network of a large variable population of mEPSC shaped synthetic mini of differing half width and amplitude providing the network the ability to find very small mini otherwise unidentified by human observers.

To complete the training set noise is added to the synthetic minis. Due to averaging of ten observed minis the template mini that goes into the creation of each synthetic mini has very little noise. This will be remedied by the linear addition of noise, which is data found from the electrophysiological recording under observation (Figure 1.1 B). The choice to take recorded samples from the recording observation stems from the desire to have the most relevant noise for the artificial neural network to learn from. Thus, 10,000 160 point sections are taken from the recording and linearly summed with the previously generated synthetic minis. Another 10,000 randomly selected 160 point sections of the recording will be used as the negative noise samples in the training set. The caveat to this method of noise addition is that if there is no recording accompanying the original recording that lacks minis (i.e. a recording in the presence of a drug – e.g. NBQX – that blocks minis) (Nikam and Kornberg, 2001) then there may be real

minis very rarely included in the training set. Because of the alignment factor, which requires a mini to be found with a peak exactly at point 60, the probability of this accidental inclusion is extremely low over the entire length of a 10 min recording in the 10000 noise samples or the 10000 synthetic mini samples at recording rates of 5000 or even 2000 samples per second. Thus, the benefit of using real noise from the actual sample under analysis proves useful in providing the network with a training set superior to one manually identified by a human. The final result is a training set with variable amplitude and width synthetic mins containing real noise from the training set under observation (Figure 1.1 C).

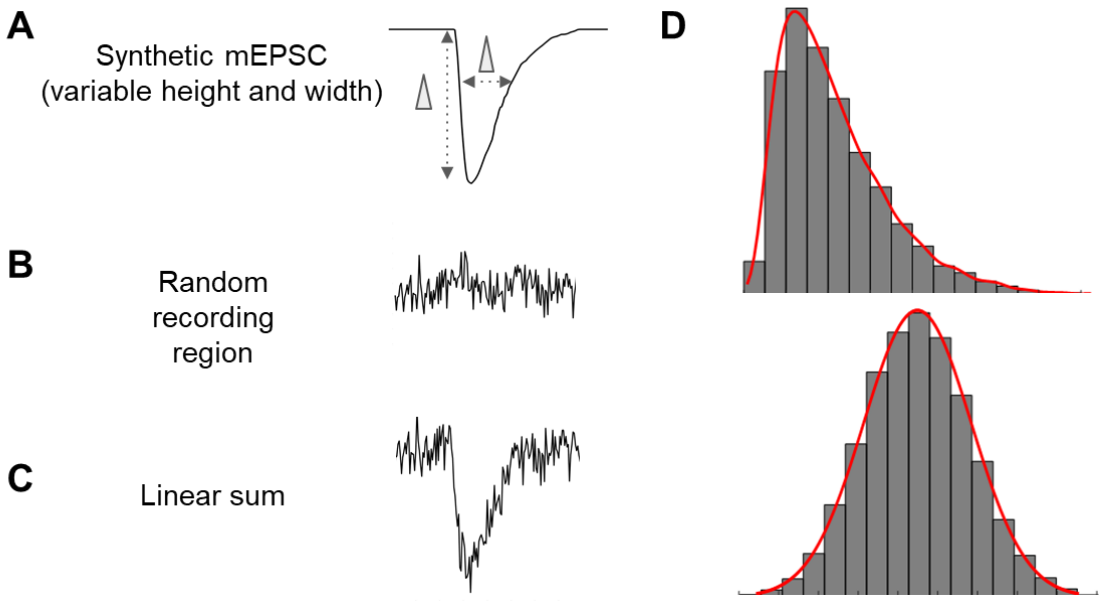

Figure 1.1. Generation of training inputs. Example of training input to be designated as 'true'. A, smooth 'synthetic' mini (160 points) is digitally added to (B) a random recorded region (160 continuous points). C, Linear sum is used as a training mini designated 'true' (value =1) in training process. Random recorded region is designated as 'false' (value = 0) D) Example Pearson distribution (top) and Gaussian distribution (bottom) See Chapter Text for details regarding this and subsequent Figures.

A standard approach using our novel training set is then undertaken to train the artificial neural network (see Figure 1.2) (Mathworks, 2020; Sejnowski, 2020; Google Research 2013; Hagan, 1996). The artificial neural network undergoes supervised learning utilizing the synthetic mini and noise training set. The network utilized is a basic feed forward network (several dozen types of ANN proved no more reliable than feed forward in testing) (Mathworks, 2020) that forms connections between nodes via a learning process that passes data in a single direction through the network, and has “backpropagation,” that is the weights of the connections between nodes are reweighted after each iteration. In order to “learn” from this set the ANN requires the addition of a key telling it when a sample contains a mini or when a sample is just noise. This key is called the target set. Normally the target set is generated by a human observer who has laboriously hand annotated which samples are true (1) and which are false (0) In this case because we have generated 10,000 samples with synthetic minis (Figure 1.2 C) and 10,000 samples of noise (Figure 1.2 A), there is no need to manually annotate the target set, and therefore an automated target set is automatically generated along with the training set. Figure 1.2 B represents a rare and unlikely example in which a real mEPSC might get included in a training set noise sample because we are utilizing real electrophysiological data from the recording under analysis. This sample is marked as a negative sample (0) because the peak of the mini is not aligned to point 60 as discussed above. It is conceivable that an extremely rare event could occur in which a noise sample has a real mEPSC aligned at point 60, and would be designated as a noise event in the training. This event, however, probabilistically happens less than 1/10,000 for a ten minute recording. If such an inclusion occurs the most likely course of the network would be to ignore the sample as an outlier as there are thousands of samples, again bringing to focus the importance of automatically generating a large training set. Each sample created with a synthetic mini is paired to an array containing 10,000 ones and each noise sample is paired to an array containing 10,000 zeroes. The network training performs the same whether this training/target data is presented to it in blocks or randomly organized, e.g.

10,000 ones/minis versus 10,000 zeros/noise or ones and zeros randomly dispersed through the training set. This may be due to the fact that the algorithm generating the artificial neural network is already chunking the data semi randomly in order to create a holdout set for which it can test itself to ensure accuracy (Google Research 2013; Hagan, 1996; Mathworks, 2020). The training follows the standard protocol utilizing gradient descent in order to minimize the difference between the target set and its output results (Moller, 1991) Upon each iteration the network is connected anew, strengthening or weakening various connections in order to provide better results (e.g. minimize the difference). Finally, the holdout set is utilized to test the network and ensure that the training has not been overly specific or overly general. Over specificity most often occurs in a neural network when not enough samples are provided, leading to a network which acts almost as a template matching algorithm only identifying exactly the inputs it has been fed as input, or when a network has been over-trained. Over generalization on the other hand occurs when everything and anything may be identified as the target waveform or shape. Overgeneralization can occur if the network is under trained (Sejnowski, 2020). In order to avoid this we have provided the network with a large training set, and have largely left the minimization efforts using gradient descent to an optimized process automated by Mathworks (Mathworks, 2020; Google Research 2013; Hagan, 1996). The neural network now having been trained can be utilized to detect minis by analyzing the confidence value output.

A neural network is thus trained by designating thousands of noisy synthetic versions of a mini as ‘true’, and thousands of randomly chosen sections of the recording as ‘false’ (all 160 pts). Once trained, one can test an input (a 160 point recording section) by feeding it into the network. The output, for that 160 section input, is a single value, called a ‘confidence value’; a value between 0-1, which is the trained networks measure of the likelihood that the input is a ‘true’ event (Figure 1.3 C and D).

TRAINING PROTOCOL

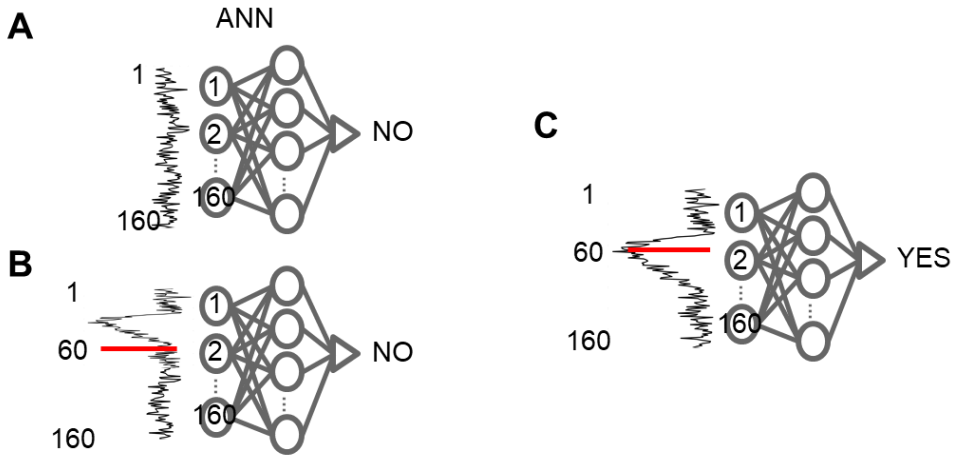

Figure 1.2. Training methodology utilizing previously generated 160 point “synthetic mini” and randomly selected 160 point noisy electrophysiological data sample from recording. Synthetic mini’s and randomly selected 160 point data are associated with a target array automatically upon generation. Each 160 point sample is then separately fed into the input layer of the network, which undergoes supervised learning using the target array to make corrections via a gradient descent process. A and B) noise and data containing minis with peaks not aligned at point 60 are associated with a 0, which during training will cause the network to learn to output low CV when fed samples similar to these. C) Synthetic mini’s aligned with their peak exactly at point 60 out of the 160 point data array are associated with a 1 (YES), which will cause the network to learn to output high CV when fed similar samples.

The ANN final output is called a confidence value (Figure 1.3 C and D). Every point in an electrophysiological recording is analyzed, using the surrounding 160 points of data (59 points before and 100 points after), step wise so that the confidence value output is a continuous set with length equal to the recording. Technically this is done prior to analysis by “chunking” the data by creating a matrix which contains 160 point samples for every data point. These samples are then each individually run through the neural network. This approach provides us with a point for point confidence value trace that can be aligned with the electrophysiological recording. When a 160 point data sample is input into the ANN with a mEPSC peak aligned at point 60 in that sample (Figure 1.3 A red box), the network takes this data and feeds it in a unidirectional manner through the connected nodes (Figure 1.3 B). The sample “activates” the network in a certain way, or in other words the sample data is passed through the network where it is found to be more similar to positive learned cases or negative learned cases. For example, if a mEPSC 160 point sample containing a peak at point 60 was passed through the network, the network would be activated in a way similar to a positive learned case and output a high degree of confidence, rated from 0 to 1 where 1 represents 100% confidence that the sample is a positive case or in other words a true mEPSC (Figure 1.3 C and D red arrows). The continuous nature of the confidence values allows for the observer to see how the network increases confidence as the peak of the mini becomes more aligned (Figure 1.3 C), forming a confidence value peak at the same point in the electrophysiological data that a mEPSC peak exists (Figure 1.3 C and D red arrows). Alternatively, if there is no mEPSC or the mEPSC is not peak aligned (Figure 1.3 A grey box) the confidence value will be lower, eventually reaching close to 0 when no mEPSC is in the 160 point sample at all (Figure 1.3 C grey arrow).

This confidence value data is substantially less noisy than the original electrophysiological recording and therefore can be used to obtain the exact location of the mEPSC in said recording. We utilize a simple peak finding algorithm (Mathworks, 2020) to find the peaks in the confidence values, providing us the exact location of mEPSC. The peak finding

algorithm has various criteria for deciding what is a peak (such as width, threshold from nearest neighboring points, total peak height, among others) (Mathworks, 2020), but two key criteria which can limit the number of false positives are the peak threshold (namely how high the confidence value peak is versus the surrounding background) and the peak width (the full width of the peak). By changing these variables the observer can control the permissiveness or rigidity of the final detection of mEPSC because each confidence value peak representing a single mEPSC has threshold and width characteristics that remain consistent. This effective detection paradigm is tested in chapter 2 in order to determine the overall effectiveness of the ANN in finding mEPSC.

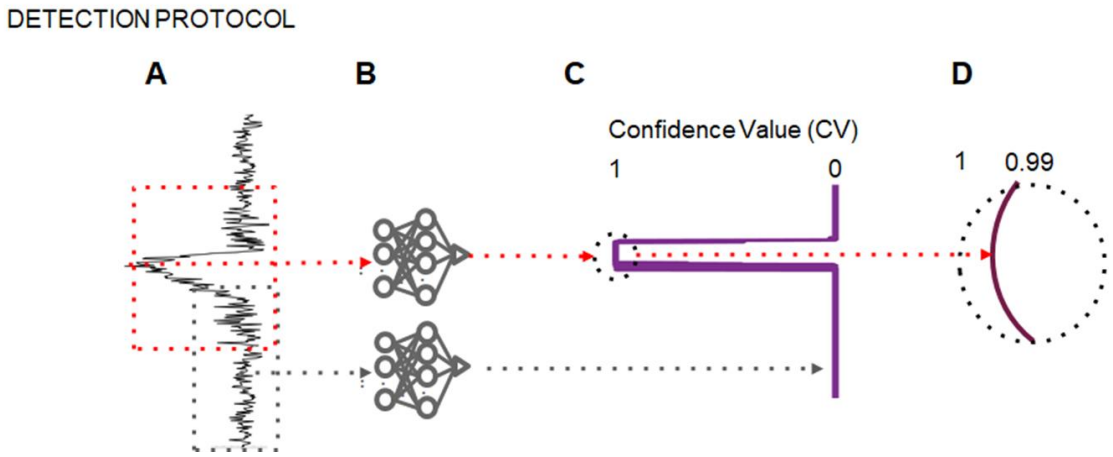

Figure 1.3. Detection protocol: Illustration of the final output value of the artificial neural network after training. A) Example electrophysiological data input entered into the neural network. Red dotted box: a 160 point sample with a peak aligned at point 60; Grey dotted box: a 160 point sample with no mEPSC B) Each 160 point sample is fed separately into the neural network (only two samples are shown here for visual clarity, but there is one 160 point sample for every point in the recording) C) Confidence value (CV) outputs from the network aligned to point 60 of each 160 point sample (notice the peak aligns with the sample whose point 60 out of 160 is at the mEPSC peak D) Enlarged CV region with value close to 1.

Results

In order to determine the quality and effectiveness of the artificial neural network in detecting mEPSC in noisy electrophysiological data a testing method was conceived. Rather than compare against a human observer initially, who are unreliable even when highly trained, it was believed that a more effective approach would be to utilize an artificially constructed test set. The test set is constructed somewhat similarly to the training sets described above, differing in several critical components. To construct the set an electrophysiological recording is obtained in the presence of NBQX, to block AMPA receptor transmission and thus mEPSC (Nikam and Kornberg, 2001). This noise without any minis was digitally summed with synthetic minis constructed similar as in the learning paradigm (see chapter 1 page 10-11). The key factor here is that because the NBQX recording has no real mEPSC because NBQX is an effective AMPA receptor antagonist (Nikam and Kornberg, 2001), the only detections a program or human observer should find are the synthetic minis placed at known locations throughout the test recording. Thus, we can compare how well the ANN detected minis versus the known number and location of these minis. Further, we can manipulate the size, shape, and location of these synthetic minis to test the robustness of the ANN. See Figure 5 and 6 (magnified version of Figure 5) to appreciate the effectiveness of the ANN. Figure 5 A/Figure 6 A represent the orange synthetic minis overlaid onto a blue NBQX trace that has no real mEPSC. Figure 5 B/Figure 6 B show the linear sum of the synthetic minis and NBQX trace, where orange dotted lines allow the observer to see the alignment of the synthetic minis and nbqx trace to the detection of the ANN in the linearly summed trace. Figure 5 C/Figure 6 C show the confidence values (as seen in Figure 1.3) peaking where there are synthetic minis. Green dots represent positive detections, while orange filled in represents a false positive, and orange empty circle represents a false negative. Figure 5 and 6 present a visually striking image of the ANN's effectiveness to detect synthetic minis in real NBQX electrophysiological recordings. Chapter 2 will discuss the quantification of these results.

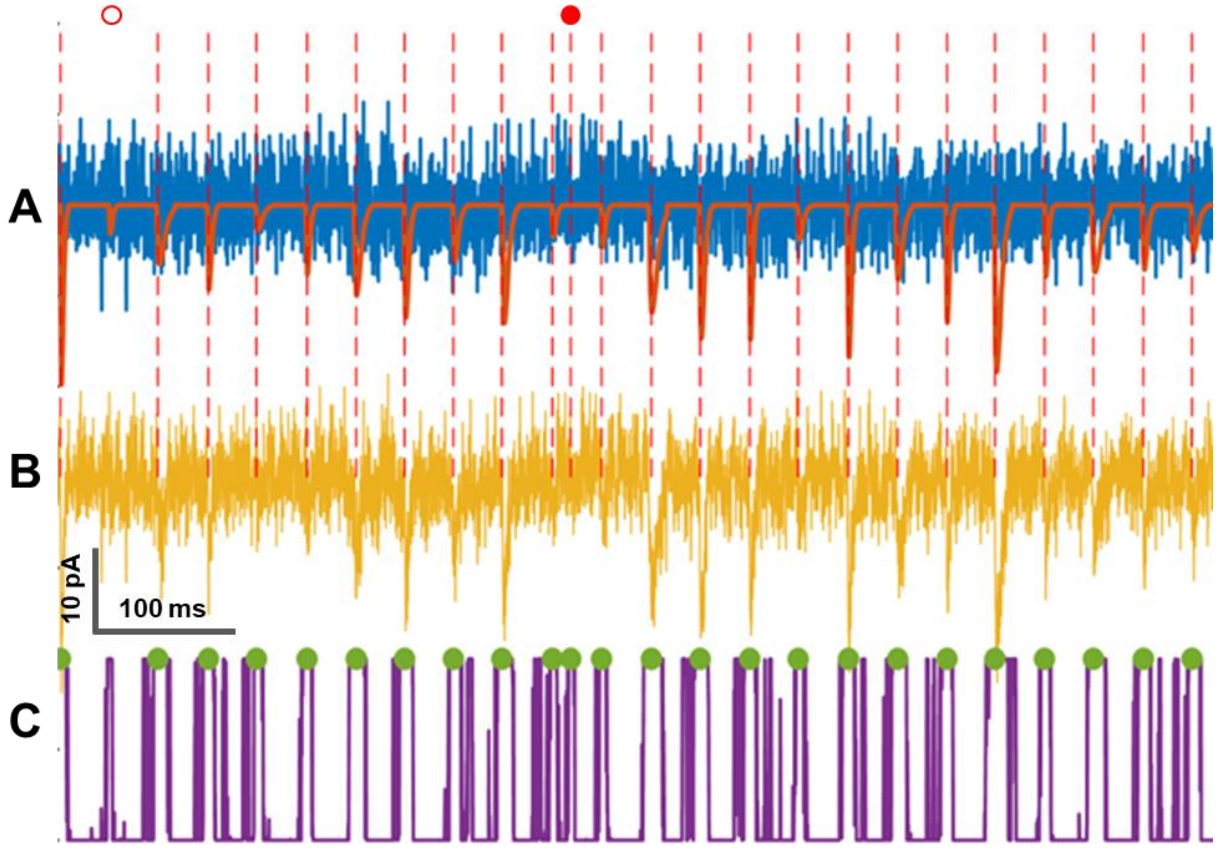

Figure 1.4. Detection of synthetic minis superimposed on electrophysiological recording noise. A) Blue, electrophysiological recording in NBQX; red, evenly spaced synthetic minis with variable amplitudes and widths B) Yellow, linear sum of blue and red (ANN input data). C) Purple, ANN confidence value outputs aligned to the input data. Peak-finding MATLAB program applied to purple trace generates detected peak (green symbol). Red dashed line, is placed based on green symbols. Note alignment between detected mini (green symbol) and placed synthetic mini. Open orange circle, false negative mini identification by the ANN. Closed orange circle, false positive mini identification by the artificial neural network.

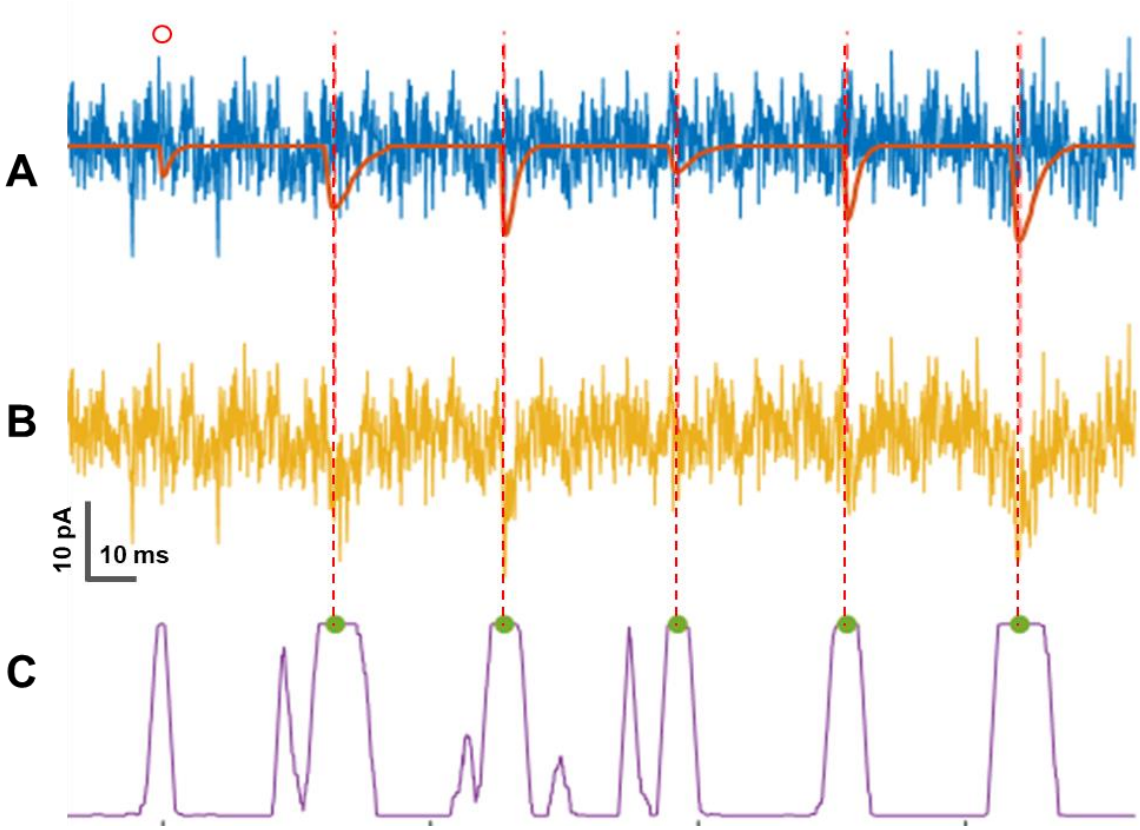

Figure 1.5. Enlargement of Figure 5. A-C) same as in Figure 5. Note CV peak value (green symbol), used to identify minis, and aligns well to the peak of the mini. CV peaks identified by MATLAB peak finder function, using both peak prominence threshold (~0.99) and width (~10 ms) to find CV peak (green symbol). Note some purple regions have 'peaks' that do not satisfy criteria and are thus not designated as a true peak.

Discussion

Visually these results demonstrate clearly how a novel approach to training artificial neural networks utilizing artificially constructed inputs based on real mEPSC can provide a fast and reliable method for training ANN. This process of training the network is the critical step in moving mini analysis from a laborious error prone process involving biased human observers to an altogether unbiased computational method of detection and analysis. We started this training paradigm with the initial step of creating an artificial mini. This allowed us to utilize very small mEPSC in the training we would not have otherwise been able to use or detect. We next realized that an important component of the detection would be the alignment of the waveform, which led to the decision to place training artificial minis at the exact same peak aligned point for each training sample. This decision ended up aiding the process in two ways. First, this produced confidence values that would also attain their peak values around the moment a real recorded sample aligns its peak at point 60 in the 160 point sample being analyzed. Second, this allows us to know precisely where the peak and baseline of every mini found is by using information gained from the confidence value peak finding (this will be discussed further in chapter 3). Ultimately, we find that artificial neural networks trained with artificially constructed data prove to be effective in detecting small waveforms in noisy electrophysiological data. Further, this training paradigm could likely be utilized by other researchers looking for different waveform signals in electrophysiological data such as EPSC, action potentials, or Spikes (see conclusion for more discussion on this topic).

References

Bekkers JM., Richerson GB. & Stevens CF. (1990). Origin of variability in quantal size in cultured hippocampal neurons and hippocampal slices. Proceedings of the Nationial Academy of Sciences of the USA 87, 5359-5362.

Findpeaks. www.mathworks.com. Retrieved 3rd June 2020. https://www.mathworks.com/help/signal/ref/findpeaks.html

Google Research, “TensorFlow: Large-scale machine learning on heterogeneous systems,” 2013.

Hagan M.T., H.B. Demuth, & M.H. Beale, Neural Network Design, Boston, MA: PWS Publishing, 1996, Chapters 11 and 12.

Isaacson JS, Walmsley B. Counting quanta: direct measurements of transmitter release at a central synapse. *Neuron*. 1995;15(4):875-884.

Malinow R, Tsien RW. Presynaptic enhancement shown by whole-cell recordings of long-term potentiation in hippocampal slices. *Nature*. 1990;346(6280):177-180.

Moller M F. “A scaled conjugate gradient algorithm for fast supervised learning,” Neural networks, 1991.

Multilayer Shallow Neural Network Architecture. www.mathworks.com. Retrieved 18th April 2020. www.mathworks.com/help/deeplearning/ug/multilayer-neural-network-architecture.html

Nikam SS, Kornberg BE. AMPA receptor antagonists. *Curr Med Chem*. 2001;8(2):155-170.

Paulsen O, Heggelund P. Quantal properties of spontaneous EPSCs in neurones of the guinea-pig dorsal lateral geniculate nucleus. *J Physiol*. 1996;496 (Pt 3)(Pt 3):759-772.

Sejnowski TJ. “The Unreasonable Effectiveness of Deep Learning in Artificial Intelligence.” Proceedings of the National Academy of Sciences, 2020, pii. 201907373.

Van Eycke YR, Foucart A, Decaestecker C. Strategies to Reduce the Expert Supervision Required for Deep Learning-Based Segmentation of Histopathological Images. *Front Med (Lausanne)*. 2019;6:222.

CHAPTER 2: Quantification of artificial neural network effectiveness at detection of mEPSCs

Introduction

The importance of quantifying the effectiveness of an automation of a manual process cannot be understated (Koen et al., 2017; Mathworks, 2020; Sejnowski, 2020; Google Research 2013). One of the key aims of this project is the attempt to replace a laborious and time consuming process with a computational method that obtains accuracy superior to human data analysis. To demonstrate the performance of the artificial neural network detection of mEPSC we undertook several types of analysis: comparison of true positives versus false positives, comparison over different amplitudes (Koen et al., 2017, Mathworks, 2020), comparisons of true positives versus false discovery rate (Yoav, 1995), and finally a head to head comparison between a highly trained human observer and the ANN system. In all these cases we observe a clear and unequivocal improvement of the ANN at detecting mEPSC at rates better than a human observer or any other currently available computational method.

Results with Materials and Methods

In order to quantify the effectiveness of the ANN in detecting mEPSC we utilized a Receiver Operator Characteristic Curve (ROC curve) method (Koen et al., 2017). Simply this method plots the true positive rate, the number of found true cases over know true cases, versus the false positive rate, the number of false cases over total possible false cases. The curve is made by individually plotting the true positive rate versus false positive rate at different sensitivity levels of the ANN's detection of synthetic mEPSC in NBQX electrophysiological data (see chapter 1 page 10-11 for details on the test set paradigm). In our case we modulated the sensitivity of the network by changing the confidence value peak threshold from 0 to 1. This produces a curve (figure 2.1 red) where at higher confidence values e.g. above 0.9 (left side of the curve) the true positives remain high while the false positives remain low. At high confidence value thresholds some true positives are unable to be detected in order to obtain a very low

false positive rate, while at lower confidence value thresholds one eventually obtains detection of all points as “positives” resulting in a 100% false positive rate represented by 1 on the X axis while also detecting all true positives. This modulation of the confidence value threshold can be thought of in the same way as a sieve with finer or coarser mesh: the higher the confidence threshold the less passes through to be ultimately detected, while at lower confidence thresholds much more passes through. An observer can use the ROC curve to choose an appropriate confidence value threshold for their data: one in which a high level of true positives are detected and few false positives are found. In general for the data utilized in this dissertation a confidence value of 0.95 to 0.99 was found to minimize the distance of the ROC curve to the far left corner (a perfect result: 100% true positives and 0% false positives). Finally, we can compare ROC curves and their area under the curve of different methods as a standard way to interpret the variable effectiveness of different methods in automatically detecting mEPSC (Pernía-Andrade et al., 2012). Figure 2.1 shows the ANN red curve (mean ROC of 10 individual recordings) versus the previously published most effective computational method for detecting mEPSC from the Jonas lab (Pernía-Andrade et al., 2012). Notice the contrast between the two curves as the ANN outperforms the convolution method (28 % improvement as calculated by area delimited by the ROC curve and the unity line). This should perhaps not be surprising as the power of artificial neural networks to effectively analyze data has become clear within the last several years. What may be surprising is the overall effectiveness in its detection, and the power to detect small minis (<5 pA), which will now be discussed.

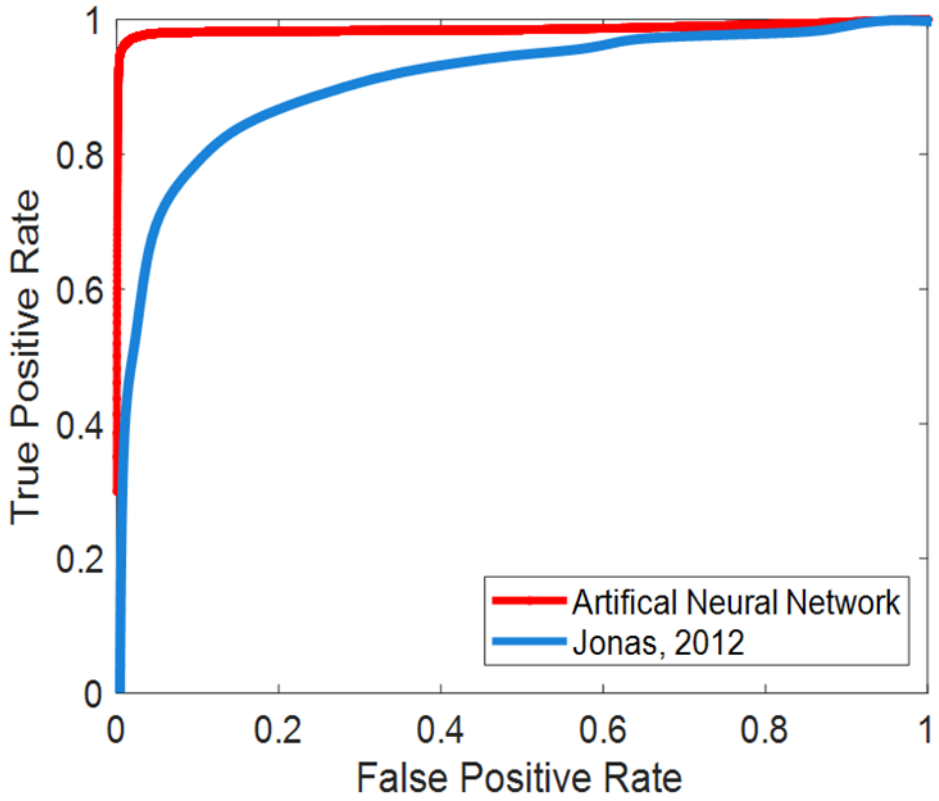

Figure 2.1. Receiver operating characteristic of the trained mini detection artificial neural network (red) to identify False Positives Rate (FPR) versus True Positive Rate (TPR). Red) The ROC curve generated by the average of 10 experiments tested on synthetic mini compared to Blue) For comparison, the ROC for a deconvolution method to identify minis (Jonas, 2012). Each point of the ROC represents the FPR vs TPR at a single confidence threshold from 0-1 for the artifiicial neural network.

Another important question is: how effective neural networks are at detecting small mEPSC? As stated in the introduction one of the aims of this project was to detect very small mEPSC, smaller even than a human observer could detect in noisy data. To answer this question, we constructed test sets similar to that used for figure 1.4-2.1, but instead of utilizing Pearson distributed amplitudes of minis as before, the network was tested with uniform distributions of single amplitude synthetic mESPC. This allowed us to determine the ROC curve for each individual amplitude from 15 to 1 pA. Figure 2.2 show that above 6 pA the network performs extremely well (with the ROC curve area under the curve reaching nearly 100%). Note also that even at 3 to 5 pA well below normal human detection levels (normally 8-10 pA Isaacson and Walmsley, 1995; Malinow and Tsien, 1990) a fair rate of true positive compared to false positives may be obtained. These very small mEPSC could not be detected by a human observer reliably (see figure 2.4 for further comparison versus a human observer). This is because at some point the noise overlaps the real mEPSC in amplitude, but also because it becomes impractical to go point by point by eye in order to attempt to find anything (small or large) as a mini. Only in the case of a recording containing stimulation in which case an event as small as a mini will occur in an exact known time frame, can human observation detect events of this small amplitude. This precludes recordings of spontaneous activity. The ANN has no such differentiation and can be used for any recording to detect these small mEPSC.

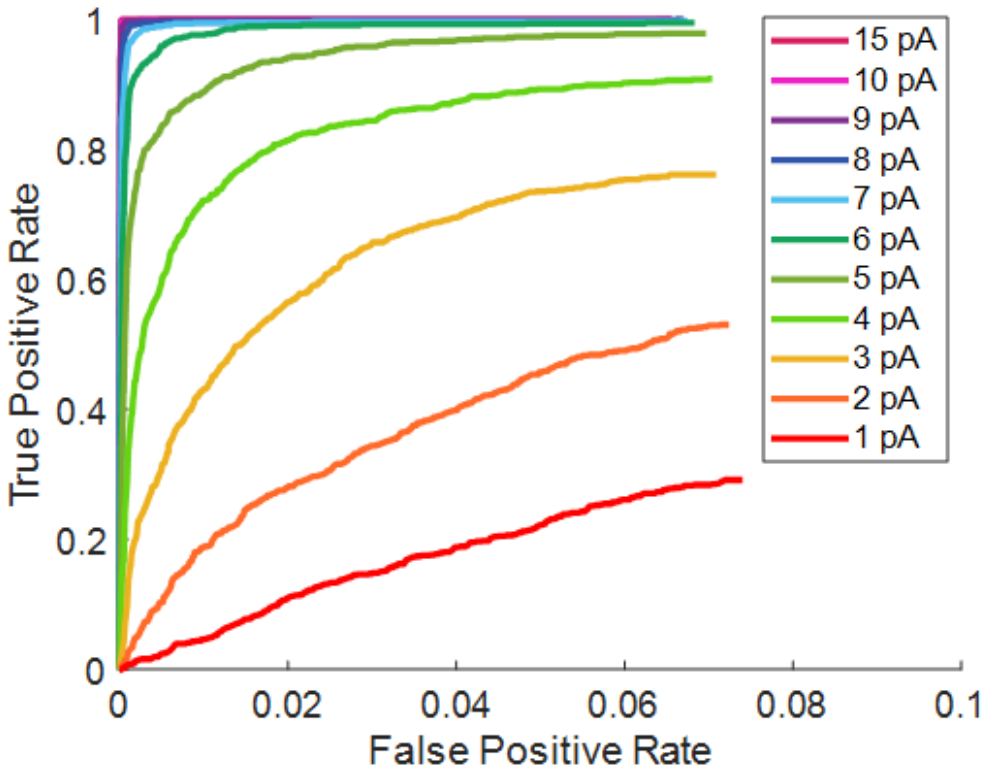

Figure 2.2. ROC curves showing True Positive Rate vs False Positive Rate performance of ANN tested to detect minis of different amplitudes. (ANN was trained with a Pearson's distribution of amplitudes). Curves indicate average of 10 electrophysiological recordings. For each recording, ~5,000 synthetic minis of indicated amplitude were digitally added to recording noise. Notice high performance on small mini's with Amplitude 4-8 pA.

We also wished to calculate the fraction of false positives as compared to true positives. We want to know not just the false positive rate (which considering the large number of points could simply be a reflection of a large sample), but rather how meaningful the data we are collecting really is. In other words, we want to be sure that the vast majority of the detections we are making are true positives and not false. False discovery rate is another method of comparing the effectiveness of a computation system to detect true versus false cases. False discovery rate is defined as the number of false positives over the number of false positives and true positives (Yoav, 1995). Thus, false discovery rate allows an observer to obtain knowledge of the percentage of likely false positives in the total number of detected observations. False discovery rate gives an observer a sense of how likely an observation is to be a false positive at a certain confidence value threshold (sensitivity). In order to obtain the false discovery rate curve, true positives were plotted versus false discovery rate for each individual threshold from 0-1. The subsequent curve shows that a high degree of confidence can be placed in each individual observation as even at quite low confidence values the false discovery rate remains below 10%. Thus, an observer can trust this computational method to deliver data that are reliably real mEPSC.

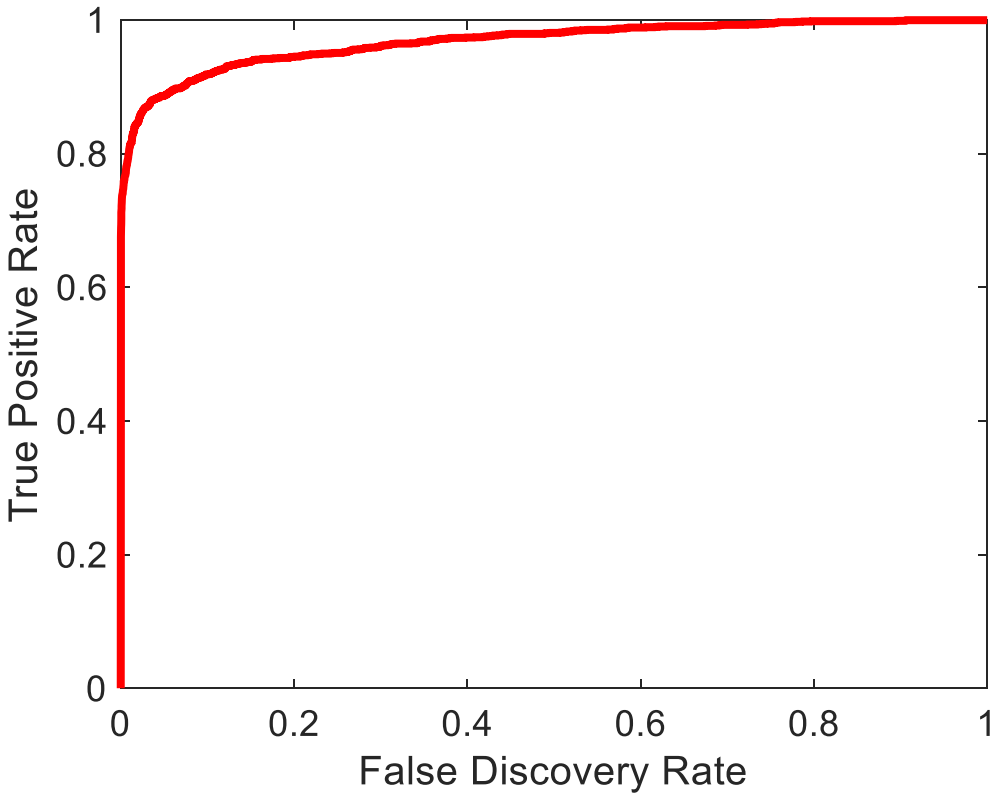

Figure 2.3. . Plot of True Positive Rate (TPR) versus False discovery Rate (FDR). The FDR is a useful metric to show the observer the proportion of detected minis are likely to be false positives.

Finally, in order to demonstrate the improved performance of our method compared to currently utilized methods, we compared artificial neural network analysis performance to human observers. We contend that the best test of the ANN in terms of effectiveness is in fact observing trials in which the network detects synthetic mEPSC in NBQX data (see Figure 3.1). While usually human observation is considered the “gold standard” for which an automated computational method should be compared, in the case of mEPSC detection human detection leaves much to be desired. Nonetheless we undertook a comparison in order to show not only the improvement in detection one observes from utilizing ANNs to detect minis, but also to demonstrate some of the issues human observation has in detecting these small electrophysiological waveforms in noisy recording data. Some of the issues of comparing humans are that they are trained differently on different data so that one observer cannot be switched for another (inter observer bias) (Burgess, 2011). But worse as we show here, even if a single human observer analyzes a dataset their own bias can cause intra observer analysis contamination (Burgess, 2011). To ensure that system users would have confidence in the ANN we compared the effectiveness of the system to a highly trained observer. The highly trained observer was given an NBQX recording with synthetic mEPSC placed at random intervals. The observer was blind to the data and given no information about the number or placement of mEPSC. The performance of the human (O and X symbols) is compared to that of the ANN in Figure 2.4. On first observation (Figure 2.4 O) the human observer performed well below the ANN in terms of number of true positives found, as well as having a higher false positives rate. In summary the human observer was not able to find as many mEPSC and also detected more false positives. Noticing that the observer particularly missed many of the smaller synthetic mEPSC, the observer was asked to analyze the same data again, given the information that she or he had failed to identify small mEPSC. She or he on this second attempt would look for and find small mEPSC thus reducing her/his internal threshold for what was or was not a mini. This second trial by the human observer should hypothetically increase the number of mini found at

the cost of also increasing the false positive rate. This second trial (Figures 10 X) produced a human observation that indeed found significantly more mEPSC including some smaller mEPSC but also significantly increased the false positive rate. Notice that in both trials the human observer falls well below the ROC curve meaning that even at low confidence value thresholds the ANN still outperforms human observers. This means that a user of the ANN method should be able to obtain more mESPC that are real from their data than a well-trained human observer could, while also being more certain that the ANN has a lower false positive rate than that same human observation would have produced.

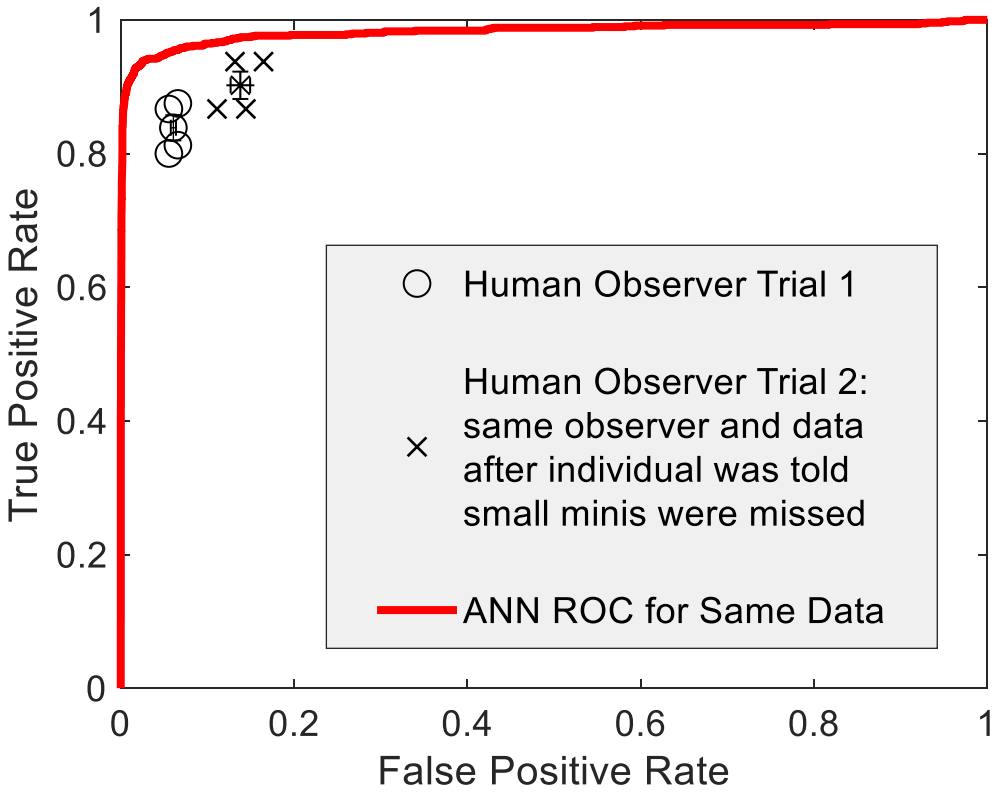

Figure 2.4. ANN ROC curve (red) of synthetic mini detection in noisy electrophysiological recording compared detection of the same data by a trained human observer (symbols). Black circle symbols (high sensitivity), initial detection (TPR and FPR) by observer of 4 continuous 2000 ms sections. Black X symbols (low sensitivity), subsequent detection by observer after being told that too few true minis were detected on initial detection session. Symbols with error bars (SEM) represent means of each session. Note that in all cases the human TPR and FPR fall below the ANN performance. For this example, synthetic mini amplitude (mean = 10 pA, signal) and noise amplitude (SD=1.2 pA, noise).

Discussion

We can conclude from the observations presented that artificial neural networks provide increased performance over both human analysis of mEPSC electrophysiological data, but also other computational methods. Speed, reliability, performance are all attributes that the ANN method has over other detection methods. Further, these data show that detection of small mEPSC is not only possible with ANNs, but relatively effective especially considering the past impossibility of detection of these small minis in spontaneous un-stimulated recording settings. This tool should then not only speed and improve mini analysis, but also provide new insights into data. Open questions remain about how these small minis will look compared to larger sized minis, as well as their frequency, or even their electrophysiological/synaptic importance. To our knowledge no one has yet fully appreciated/studied such small mEPSC in spontaneously recorded electrophysiological data. It is our hope that with tools such as ANN more insight into small mEPSC might be gained.

References

Burgess AE. Visual perception studies and observer models in medical imaging. *Semin Nucl Med*. 2011;41(6):419-436.

Koen J. D., F. S. Barrett, I. M. Harlow, and A. P. Yonelinas, “The ROC Toolbox: A toolbox for analyzing receiver-operating characteristics derived from confidence ratings.” Behav. Res. methods, vol. 49, no. 4, pp. 1399–1406, Aug. 2017.

Google Research, “TensorFlow: Large-scale machine learning on heterogeneous systems,” 2013.

Isaacson JS, Walmsley B. Counting quanta: direct measurements of transmitter release at a central synapse. *Neuron*. 1995;15(4):875-884.

Malinow R, Tsien RW. Presynaptic enhancement shown by whole-cell recordings of long-term potentiation in hippocampal slices. *Nature*. 1990;346(6280):177-180.

“Neural network performance - MATLAB crossentropy - MathWorks Nordic,” Retrieved 3-July-2020. http://se.mathworks.com/help/nnet/ref/crossentropy.html.

Pernía-Andrade A.J., Goswami S.P., Stickler Y., Fröbe U., Schlögl A., Jonas P. A deconvolution-based method with high sensitivity and temporal resolution for detection of spontaneous synaptic currents *in vitro* and *in vivo*. Biophys. J. 2012;103:1429–1439.

Receiver operating characteristic (ROC) curve or other performance curve for classifier output (perfcurve function). Mathworks Inc. Retrieved online 3rd June l 2020. www.mathworks.com/help/stats/perfcurve.html

Sejnowski TJ. “The Unreasonable Effectiveness of Deep Learning in Artificial Intelligence.” Proceedings of the National Academy of Sciences, 2020, pii. 201907373.

Yoav B., Hochberg, Y (1995). "Controlling the false discovery rate: a practical and powerful approach to multiple testing" (PDF). *Journal of the Royal Statistical Society, Series B*. 57 (1): 289–300.

CHAPTER 3: Amplitude detection utilizing output features from the artificial neural network

Introduction

Amplitude detection is one critical component of the reporting and detecting of mEPSC (Auger and Marty, 1997; Simkus and Stricker. 2002). Along with rise time and frequency, amplitude is one of the fundamental characteristics of mEPSC that provide observers information about the neuron being recorded (Otmakhov, 1993). In order to determine the Amplitude of a detected mEPSC, we used a mixed methodology to find a baseline and peak in the detected mini. What is essentially novel in our determination of amplitude is in how we detect the baseline, which utilizes information gained from the artificial neural network via its output: the confidence values (Koen, 2017). We then proceeded to compare the known amplitudes of artificial mEPSC with detected findings to demonstrate an effective detection rate of amplitude sizes.

Materials & Methods

First, since the mEPSC is aligned due to the operation of the ANN, we know that the peak will be at position 60 out of a 160 point window. The peak detector (Matlab, 2020) also provides us with a valuable piece of information namely the width of the confidence value peak. This width represents when the ANN began to increasingly gain confidence that a positive detection of a mEPSC was occurring. From this confidence value peak width (figure 3.1 B) an observer can obtain information regarding where the baseline of a peak occurs. The width obtained from the confidence value peak finding (see chapter 1 methods Confidence Values) is then utilized to find the middle point of the baseline. An average of 5 points on either side (for a total of 10 points) is taken at a distance from the peak determined by the peak width of the confidence value peak for that mini (figure 3.1 A black bar). This ensures an accurate baseline far enough away from the drop in the mini peak, but as close to the beginning of the mini as possible. Generally the smaller the baseline and the closer the baseline is to the area of

measurement the less noisy the final baseline subtracted measurement will be (Malinow, personal communication). Once a baseline is taken, using the knowledge that the peak is aligned at point 60, a 3 point average of maximum peak around CV-identified peak is taken to determine the amplitude (figure 3.1 right). The maximum is then subtracted by the baseline to obtain the final amplitude measurement. While this measurement is very simple in some ways (simply a max-baseline linear calculation), the use of the ANN confidence value output improves the accuracy of the baseline targeting, while the peak alignment strategy enables easier more precise measurement of the maximum peak value.

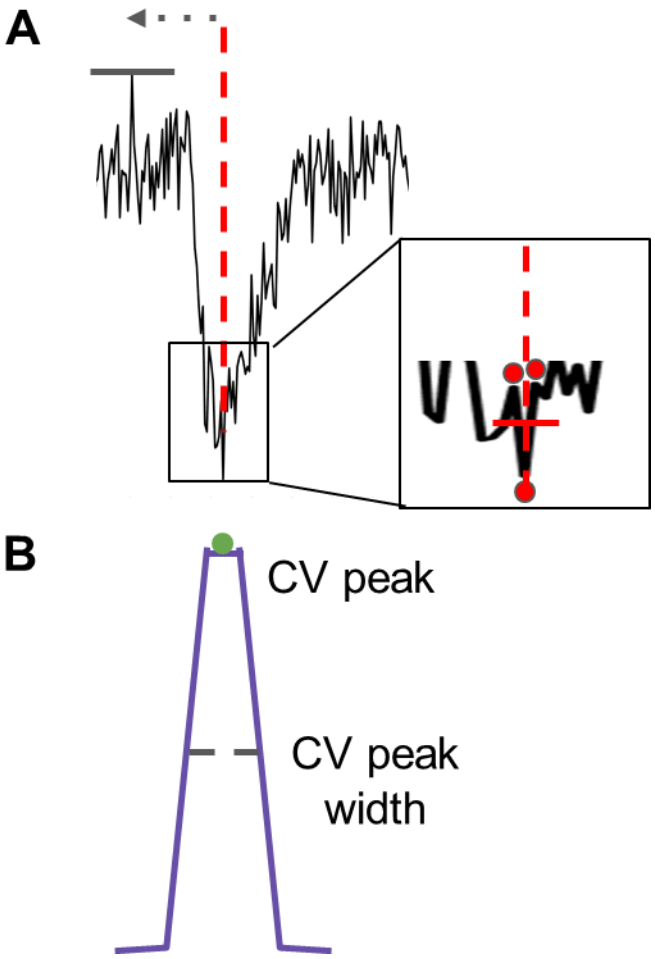

Figure 3.1. Amplitude detection of the peak using a mixed methodology to find a baseline and peak in the detected mini. A) Mini Amplitude determined using CV peak width for baseline points and 3 point average at minima for peak. Baseline is subtracted from minma value for final amplitude measure. B) Using the peak width obtained from the confidence value peak finding (see chapter 1 methods Confidence Values) a baseline of 10 points (A black bar) is taken at a distance from the mini minima determined by the peak width of the confidence value peak for that mini. This ensures an accurate baseline far enough away from the drop in the mini peak, but as close to the beginning of the mini as possible. A magnified) 3 point average of maximum peak around CV-identified peak is taken to determine the amplitude. The minima is then subtracted by the baseline to obtain the final amplitude measurement.

Results

Figure 3.2 and 3.3 are visual representations of the accuracy of the amplitude detection utilizing neural network output data. In order to compare how accurate the amplitude measurements were we generated a test set of synthetic mini with known amplitudes. We ran this test set through the ANN and the amplitude finding program to determine the detected amplitudes. We then compared detected amplitudes versus known amplitudes (figure 3.2). Notice how closely these data align to the unity line (the expected case if detection and known amplitudes were exactly the same). Averaging of three points around the peak improved amplitude detection at smaller amplitude sizes. This result clearly demonstrates the overall accuracy of this amplitude measurement method in determining the amplitude of a ANN-detected mEPSC.

Further, it is helpful to observe the distribution of known versus detected amplitudes so that one can clearly see at different amplitudes the accuracy of the amplitude finder. The histograms of the known and detected amplitudes have been plotted along with the distribution of amplitudes of the noise to give an observer an idea of the challenges of detecting amplitude size at smaller mini amplitude sizes. Notice that the known and detected histograms follow a similar pearson distribution (the synthetic mini amplitudes were set by a Pearson distribution), while the noise is symmetric around 0 (Malinow and Tsien, 1990). Mini amplitude for actual detected mEPSC seems to not fall below 0 due to the shape of the waveforms being detected by the ANN. At most amplitudes the amplitude detection is performing acceptably and will provide accurate detection of mini amplitude.

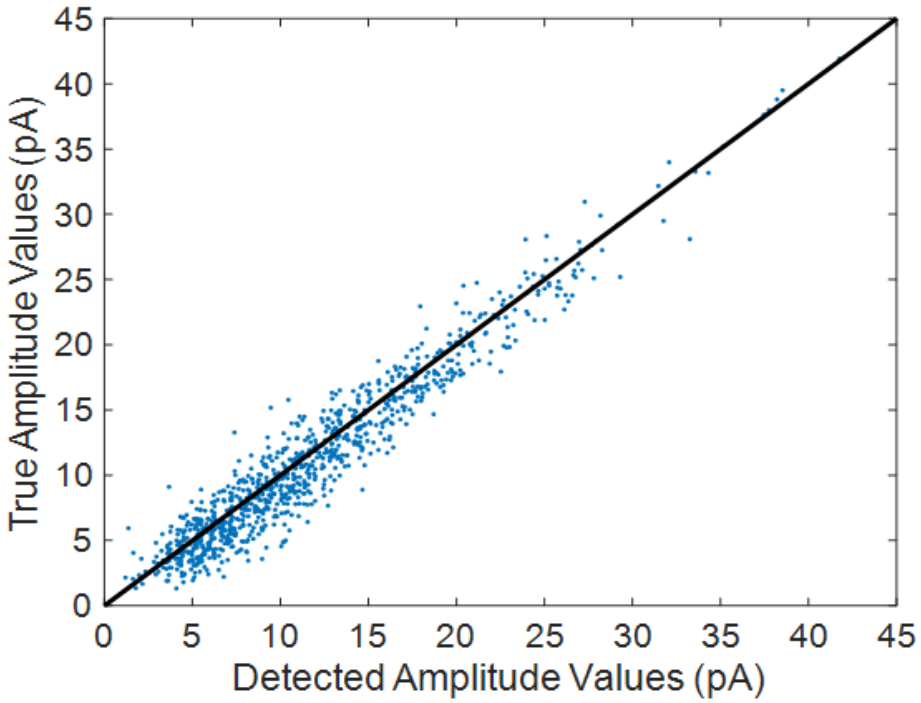

Figure 3.2. A comparison of the known amplitudes of synthetic minis overlayed onto noisy electrophysiological recordings compared to detected minis' amplitudes by the software. Each dot represents a single synthetic mini. The black line represents the unity line.

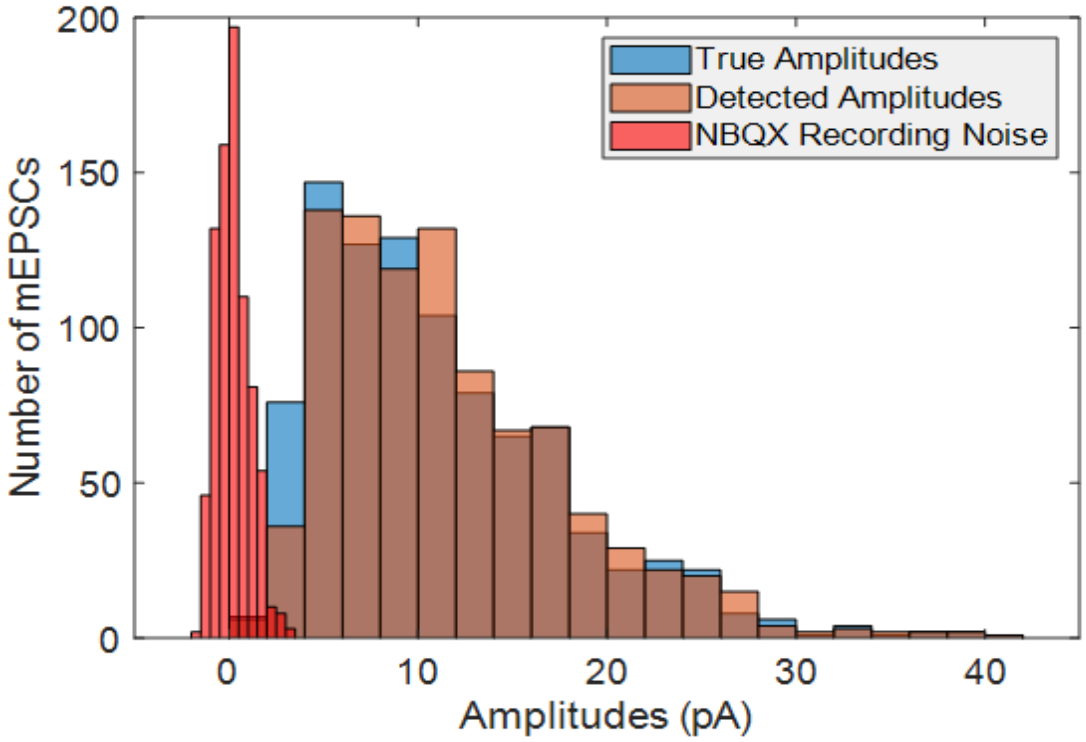

Figure 3.3. As in Figure 3.2 a comparison of synthetic minis linearly summed with electrophysiological recordings where the synthetic minis' amplitudes are known compared to the detected amplitudes of these minis by the amplitude finding software. Blue) True known amplitudes of the synthetic minis. Red) Detected Amplitudes of the mini's by the artificial neural network Dotted Line) Noise Amplitude Distribution of the electrophysiological recording on which the synthetic minis were linearly summed.

Lastly, Figure 3.4 shows the average amplitude distribution histogram of a Blue (non-nbqx) and Red (nbqx) electrophysiological recording fed into a trained artificial neural network. NBQX data because of the block of glutamate receptors should theoretically have 0 minis identified (Nikam and Kornberg, 2001), thus any identified minis can be classified as false positives giving the observer a method to judge the reliability of each amplitudes identified minis. These overlaid histograms provide two sets of information: first they provide information on the effectiveness of detecting real mini in real electrophysiological data, each recording being matched with its NBQX counterpart to provide a negative control for the ANN giving the observer a sense of the number of false positives in a ten minute recording. Notice the relatively few mEPSC found in NBQX as compared to before NBQX was added, which clearly demonstrates the effectiveness of the ANN again to detect a high rate of true positives while detecting a low rate of false positives. Secondly, these histograms again give the observer a sense of the noise amplitude distribution versus a true mEPSC distribution from real electrophysiological recordings. Notice the Pearson distribution of the real mEPSC versus the rough symmetry of the NBQX amplitudes. Together these histograms demonstrate convincingly that the ANN is a good method for analyzing noisy electrophysiological data providing not only a more rapid and reliable method, but also one that allows for detection of smaller amplitude mEPSC.

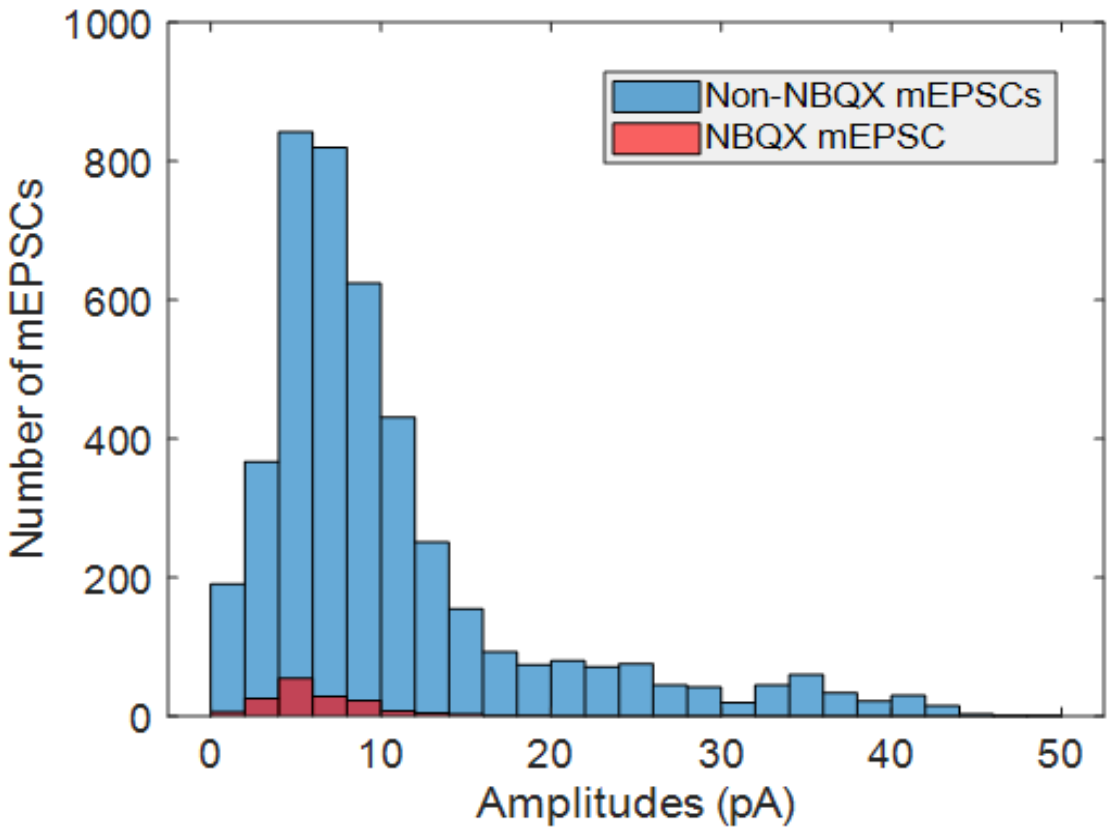

Figure 3.4. Amplitude Distribution histogram of an Blue (non-nbqx) and Red (nbqx) electrophysiological recording fed into a trained artificial neural network. NBQX data because of the block of glutamate receptors should theoretically have 0 minis identified, thus any identified minis can be classified as false positives giving the observer a method to judge the reliability of each amplitudes identified minis.

Discussion

As discussed above amplitude is utilized by researchers most often when comparing two groups of mESPC to make a quantifiable statement about two populations of neurons being recorded (Malinow and Tsien, 1990; Simkus and Stricker, 2002). It is therefore critical that these amplitude measurements should be accurate. Especially at smaller amplitudes this poses a clear difficulty because the noise overlaps amplitudes below 8 pA. These minis were previously discarded because of this challenge or not detected at all. Our utilization of the artificial neural network has enabled us for the first time in spontaneous data reliably detect such small waveforms, and therefore attempt to quantify their amplitude. Although challenging, the use of the output confidence value peak width data provides a novel tool in order to establish a baseline for which the program can then calculate a detected amplitude value (Koen, 2017; Matlab, 2020). Utilizing the confidence value in novel fashion opens up several possibilities in improving other waveform characteristic quantifications and will be applied in the future.

References

Auger, C., and Marty A.. 1997. Heterogeneity of functional synaptic parameters among single release sites. Neuron. 19:139–150.

Carnevale, N. T., and Hines M. L.. 2006. The Neuron Book. Cambridge University Press, Cambridge. 25. DeFelice, L. J. 1981. Introduction to Membrane Noise. Plenum Press, New York.

Findpeaks. www.mathworks.com. Retrieved 3rd June 2020. https://www.mathworks.com/help/signal/ref/findpeaks.html

Koen J. D., F. S. Barrett, I. M. Harlow, and A. P. Yonelinas, “The ROC Toolbox: A toolbox for analyzing receiver-operating characteristics derived from confidence ratings.” Behav. Res. methods, vol. 49, no. 4, pp. 1399–1406, Aug. 2017.

Malinow R, Tsien RW. Presynaptic enhancement shown by whole-cell recordings of long-term potentiation in hippocampal slices. *Nature*. 1990;346(6280):177-180.

Nikam SS, Kornberg BE. AMPA receptor antagonists. *Curr Med Chem*. 2001;8(2):155-170.

Otmakhov N, Shirke AM, Malinow R. Measuring the impact of probabilistic transmission on neuronal output. *Neuron*. 1993;10(6):1101-1111.

Simkus, C. R. L., and C. Stricker. 2002. Properties of mEPSCs recorded in layer II neurones of rat barrel cortex. J. Physiol. 545:509–520.

CONCLUSION

This project has made several novel contributions in the attempt to detect small electrophysiological signals in noisy recordings. While we make no claims to improving upon or inventing the artificial neural network themselves, our utilization of ANNs on this mEPSC electrophysiological data seems to be without precedent. Further, we have developed a system of utilizing synthetically generated data which appropriately mimics the waveforms of interest (namely glutamatergic mEPSCs), which we feel does in fact represent a completely novel approach to the training of artificial neural networks (Van Eycke, 2019). This new way of training a network seems to bypass some of the biggest challenges in setting up an effective ANN. First, we remove the need for human annotation of a large data set (Van Eycke, 2019; Sejnowski, 2020), which would be time consuming and defeat the aim of saving time and energy on manual observation. Second, this method allows us to introduce to the network very small mEPSC synthetic waveforms, which a human observer would not be able to annotate (Isaacson and Walmsley, 1995; Malinow and Tsien, 1990; Carnevale and Hines, 2006; Kasdin, 1995). Thus, the network will be trained and have the ability to find waveforms smaller than any human observer would detect. This gives the method a dimension beyond the simple automation of a task and moves the project in the direction of giving observers the ability to understand and observe electrophysiological data and mEPSCs in new ways. We look forward to observing these small mEPSC, their frequency, shape, and heretofore undescribed importance.

Importantly, when we tested the system to compare its output characteristics and determine its overall effectiveness in detecting mEPSC the performance exceeded even our expectations (Sejnowski, 2020; Koen, 2017). Not only did we obtain high true positive rates versus low false positives rates in tests using synthetic minis, but also by finding many mEPSC in recordings without NBQX and very few false positive mEPSC in recordings with NBQX. Equally, when we compare the ROC curves obtained by testing our system to other computational automation methods, the ANN performs better (Pernía-Andrade et al., 2012). Not

only did our method do well in comparison to other methods, but lastly and importantly, most mEPSC detection and analysis still occurs manually or partially manual with the aid of a peak finding program. Our program outperformed human observation in two trials, and is both faster and more reliable than any human observer. The false discovery rate (Yoav, 1995) should also give users confidence that the detection of small signals being made by the ANNs are reliable and accurate.

Looking to the future of detection and data analysis utilizing artificial neural networks, there are many more applications for ANN in the realm of electrophysiological data. First, new advancements in ANN will provide even greater detection ability, more reliability, and faster analysis (Van Eycke, 2019; Sejnowski, 2020). Secondly, utilizing these artificial intelligence methods for many different types of waveforms other than intracellular electrophysiological data is not only possible, but should be considered. Particularly extracellular recordings (that is spikes/field potentials) are still often manually or semi manually detected. Spike sorting and spike detection are a critical bottleneck to neuroscience data analysis as huge amounts of data can now be collected with modern probes (Hennig et al., 2019), but analysis is stymied by noisy data and the difficulties of using more generic computational processes such as peak finders or template matching systems to detect such waveforms (Hennig et al., 2019). The potential to use the mini detection ANN methods here on spikes seems achievable. All that would be required is a template of a spike and the recordings with and without action potentials. There are likely other areas of electrophysiological data analysis and detection of waveforms where we could utilize the training paradigms developed here to improve and speed up ANN creation. Ultimately, the development of this method to detect mEPSCs in noisy electrophysiological data using artificial neural networks should aid in reducing human bias in observations and analysis, improve the efficiency of data analysis, and perhaps most excitingly provide new information about data already being collected.

References

Hennig MH, Hurwitz C, Sorbaro M. Scaling Spike Detection and Sorting for Next-Generation Electrophysiology. *Adv Neurobiol*. 2019;22:171-184.

Isaacson JS, Walmsley B. Counting quanta: direct measurements of transmitter release at a central synapse. *Neuron*. 1995;15(4):875-884.

Kasdin, N. J. 1995. Discrete simulation of colored noise and stochastic processes and 1/fa power law noise generation. Proc. IEEE. 83: 802–827. Biophysical Journal 103(7) 1429–1439 1438 Pernı´a-Andrade et al.

Koen J. D., F. S. Barrett, I. M. Harlow, and A. P. Yonelinas, “The ROC Toolbox: A toolbox for analyzing receiver-operating characteristics derived from confidence ratings.” Behav. Res. methods, vol. 49, no. 4, pp. 1399–1406, Aug. 2017.

Malinow R, Tsien RW. Presynaptic enhancement shown by whole-cell recordings of long-term potentiation in hippocampal slices. *Nature*. 1990;346(6280):177-180.

Pernía-Andrade A.J., Goswami S.P., Stickler Y., Fröbe U., Schlögl A., Jonas P. A deconvolution-based method with high sensitivity and temporal resolution for detection of spontaneous synaptic currents *in vitro* and *in vivo*. Biophys. J. 2012;103:1429–1439.

Sejnowski TJ. “The Unreasonable Effectiveness of Deep Learning in Artificial Intelligence.” Proceedings of the National Academy of Sciences, 2020, pii. 201907373.

Van Eycke YR, Foucart A, Decaestecker C. Strategies to Reduce the Expert Supervision Required for Deep Learning-Based Segmentation of Histopathological Images. *Front Med (Lausanne)*. 2019;6:222.

Yoav B., Hochberg, Y (1995). "Controlling the false discovery rate: a practical and powerful approach to multiple testing" (PDF). *Journal of the Royal Statistical Society, Series B*. 57 (1): 289–300.